



Passive Mixer and Separator Integrated on a Ceramic-Based Microfluidic Device†

Ji-YUN SEON^{1,2}, YOUNG JOON YOON^{1,*}, HYO TAE KIM¹, CHANG-YEOUL KIM¹, JONG-HEE KIM¹ and HONG KOO BAIK²

¹Nano-Convergence Intelligent materials team, Korea Institute of Ceramic Engineering and Technology, Seoul 153-801, Republic of Korea

²Department of Materials Science and Engineering, Yonsei University, Seoul 120-749, Republic of Korea

*Corresponding author: Fax: +82 2 3282 7838; E-mail: yjyoon@kicet.re.kr

AJC-13279

A ceramic-based microfluidic device including a passive mixer and a passive separator was fabricated *via* a conventional low temperature co-fired ceramic process and photolithographic technique. In the mixing process, the configuration of a conventional diffusion-type passive mixer with a 500 μm channel width and 50 μm height was used. The total length of the mixing channel was 15.8 cm. The maximum mixing efficiency of the diffusion-type passive mixer was 97.3 % at a flow rate of 0.3 $\mu\text{L}/\text{min}$. In the separation process, six branch channels were arranged at the end of the pinched segment for separating different sized particles from one another. The findings confirmed that microbeads for a target channel were separated efficiently by controlling the hydrodynamic conditions of the microfluids.

Key Words: Microfluidics, Mixer, Separator, Photolithography, Low temperature co-fired ceramic.

INTRODUCTION

Many technical developments have been reported in the field of microfluidics that are based on MEMS technology for applications to biology and biotechnology^{1,2}. The emergence of plastic materials, such as polydimethylsiloxane and polymethylmethacrylate, makes it much easier to fabricate an individual microfluidic chip. However the problem of integrating each microfluidic component on a single platform for multi-functional applications remains to be solved³⁻⁵. Low-temperature co-fired ceramic materials offer a promising alternative to silicon, glass and polymeric substrates for the fabrication of microfluidic devices and microsystems for biomedical applications. Low-temperature co-fired ceramic materials are particularly suitable for use in harsh environments, for high frequency and complex microfluidic devices. Recently introduced low temperature co-fired ceramic-based microfluidic devices clearly demonstrate the advantages of the easy construction of complex 3D structures and the low cost of production⁶⁻⁹. Low-temperature co-fired ceramic is mechanically robust and chemically strong compared to the plastic materials that are commonly used for preparing biochips. It shows a good compatibility with screen printing processes, which makes it possible to integrate electronic circuits. Considering the unique properties of the low-temperature co-fired ceramic process, it could be a promising candidate for the integration of microfluidic components in 3-dimensional structures.

In this report, we provide a detailed description of a ceramic-based chip integrated with a passive mixer combined with separator and the methodology used in its fabrication. To form a microchannel and a microcavity on an low-temperature co-fired ceramic substrate, a novel photolithographic technique using a photoimageable slurry was employed. Through this technique, it was possible to control the line width of the microchannel to below 500 μm . Mixer design is critical to microfluidic applications, because turbulent flow in a microfluidic channel is almost impossible due to the limitations in the geometrical factor in a microfluidic channel. In the mixing area, a diffusion-type passive mixer with a conventional configuration was used. The mixing efficiency was calculated by tracing the change in fluorescence intensity from the inlet to the outlet region. On the other hand, in the separation area, a pinched segment configuration that was designed so as to separate particles with different sizes, was employed¹⁰⁻¹². As reported earlier, a number of systems have been developed for that purpose recently. The six branch channels were arranged at the end of the pinched segment for separating the particles. In addition, there was another inlet for the buffer solution to control the hydrodynamics of the microfluids.

EXPERIMENTAL

To fabricate the ceramic-based microfluidic chip, low temperature co-fired ceramic technology and thick film photolithography were combined. The microfluidic device was

†Presented to the 6th China-Korea International Conference on Multi-functional Materials and Application, 22-24 November 2012, Daejeon, Korea

mainly composed of Ca-modified amorphous cordierite ceramic powders $[(\text{Mg,Ca})_2\text{Al}_4\text{Si}_5\text{O}_{18}]$ with an average particle size of $2\ \mu\text{m}$. The process used in the fabrication of the ceramic-based chip has been extensively described in a previous publication¹³. The completed microfluidic device was bonded with PDMS (Polydimethylsiloxane, Sylgard 184, Dow Corning Corporation, USA) by plasma treatment (Cluster type PE-CVD system) for the transparent cover of the ceramic-based chip. We then made a hole in the polydimethylsiloxane to accommodate tygon tubes (S-54-HL, Harvard Apparatus, Holliston, MA) in the inlet and outlet ports. The tygon tubes were connected to syringes that injected the solution into the micro channel pattern uniformly using a Micro pump (Pump 11 pico plus; Harvard Apparatus, Holliston, MA).

Two types of solutions were prepared for the microfluidic experiments. One was a 2 mM fluorescein (F2456; Sigma-Aldrich, St. Louis, MO) solution in $18.3\ \Omega\text{-cm}$ Millipore water and the other was deionized water without the fluorescein for the optical quantification of mixing efficiency and separation. The solutions were then injected into the micro channel through a syringe pump at controlled flow rates ranging from 0.3 to $7.5\ \mu\text{L}/\text{min}$. The additional buffer solution in the separation area was introduced to the microchip separator with a syringe pump at controlled flow rates ranging from 0.3 to $5\ \mu\text{L}/\text{min}$. Fluorescein-coated polystyrene microbeads with a diameter of $1\ \mu\text{m}$ were also used to observe the separation phenomena after passing the suspension through the pinched channel segment. The diffused fluorescence and micro-bead images were observed by a SteREO Discovery V12 (Zeiss, Oberkochen, Germany) microscope with a MacroFire charge-coupled device (CCD) camera (Optronics, Goleta, CA).

RESULTS AND DISCUSSION

Mixing efficiency in a diffusion-driven passive mixer:

Fig. 1 (a) shows an overall image of the low-temperature co-fired ceramic-based microfluidic device including two microfluidic components, including the passive mixer and passive separator. Magnified images of the pinched channel and the mixing channel are shown in Fig. 1(b) and (c), respectively. In the mixing zone, the microfluidic channel width was $500\ \mu\text{m}$ and its height was $50\ \mu\text{m}$. The total length of the mixing channel was 15.8 cm. In the separation channel, six branch channels were arranged at the end of the pinched segment. The channel width of the pinched segment, which was connected to the outlet of the mixing channel and the inlet of the 2nd buffer solution, was reduced to $100\ \mu\text{m}$ so as to permit the efficient separation of particles using only the hydrodynamic conditions. Main drain channel is constructed to be broader than the others (branch A1 to A5) in order to reduce flow resistance in the separation channels.

The Reynolds number (Re) is 0.1 to *ca.* 2.75 in this chip geometry and it is nearly impossible to generate a turbulent flow as described above. Therefore, mixing was only achieved by the diffusion of two laminar flows in the $500\ \mu\text{m}$ mixing channel. The mixing efficiency could be calculated by measuring the change in fluorescence intensity from the inlet to the outlet. The mixing efficiency at the outlet is expressed by the following equation:

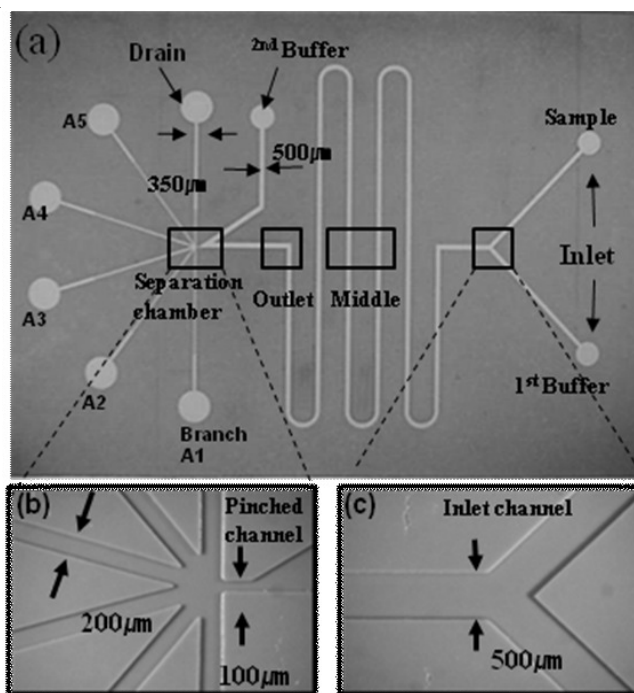


Fig. 1. Optical image of low-temperature co-fired ceramic-based microfluidic device

$$\eta = \left(1 - \frac{\int_0^A |c - c_\infty| dA}{\int_0^A |c_0 - c_\infty| dA} \right) \times 100\% \quad (1)$$

where A , c_0 and c_∞ mean the cross sectional area of the channel, the initial concentration ($= 0$) and the concentration of perfect mixing ($= 0.5$), respectively. Concentration is calculated by converting the fluorescence intensity transverse to the direction of the liquid stream flow in the mixing channel into a gray scale for extracting the numerical values. Fig. 2 shows the raw image data for the fluorescence intensity from inlet to outlet with the change in flow velocity. In the inlet region, a clear interface between the fluorescein solution and deionized water was observed because laminar flow was maintained without mixing. However, the boundary of the laminar flow was blurred as the result of the diffusion of two solutions at the interface. The concentration gradient obtained from different flow rates was at a minimum when the flow rate was $0.3\ \mu\text{L}/\text{min}$, which was the minimum flow rate in this experiment. This results indicate that the mixing in the microfluidic channel was efficiently driven by the diffusion of the two solutions. Fig. 3 shows the mixing efficiency calculated using eqn. 1 with the change in flow rate. At a flow rate of $0.3\ \mu\text{L}/\text{min}$, the mixing efficiency was maximized, reaching a value of 97.3%. As the flow rates increased, the mixing efficiency decreased linearly.

Separation of microbeads through the pinched channel:

In the low-temperature co-fired ceramic-based passive device, the separation of microbeads was achieved by controlling the flow rate distributions to each branch channel. The flow rate at each branch was dependent on the flow rate of the buffer solution that was injected into the pinched channel. Flow

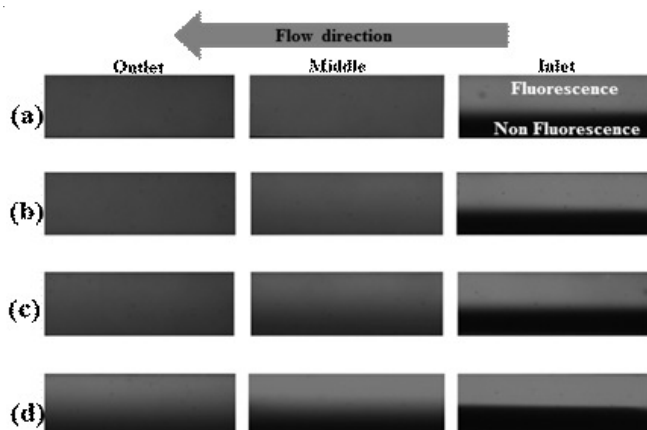


Fig. 2. Fluorescence intensity transverse to the direction of stream flow at different mixing channel regions with the change in flow velocity. The flow rate was (a) 0.3 $\mu\text{L}/\text{min}$, (b) 1 $\mu\text{L}/\text{min}$, (c) 2 $\mu\text{L}/\text{min}$ and (d) 7.5 $\mu\text{L}/\text{min}$

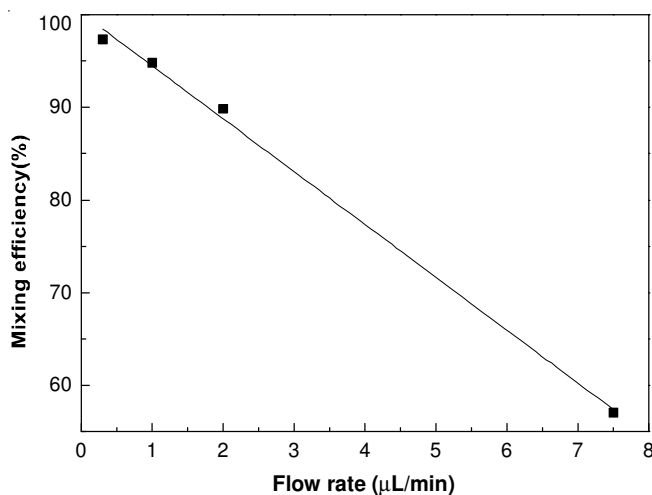


Fig. 3. Mixing efficiency with a change of flow rate from 0.3 to 7 $\mu\text{L}/\text{min}$

resistance by adjusting the width, depth, and length of the pinched channel dimensions was a major factor in determining the hydrodynamic behavior of the microbeads. Fig. 4 shows the fluorescence image in the separation region with a change in flow rate of the 2nd buffer solution. It was confirmed that the main stream after passing through the pinched segment was distributed differently as the result of the change in the flow rates of the 2nd buffer solution. This suggests that passive separation can be achieved by only the control of hydrodynamic force.

Based on the microfluidic behavior in the pinched segment with different hydrodynamic forces, an actual separation test using micro-particles in the low-temperature co-fired ceramic-based chip was performed. Fig. 5 shows that the separation phenomena of 1 μm microbeads as a function of the flow rate of the 2nd buffer solution. The flow rate of the main stream including microbeads was fixed at 0.5 $\mu\text{L}/\text{min}$. When the flow rate of the buffer solution was 0.5 $\mu\text{L}/\text{min}$, the microbeads mainly passed through the branch 1, 2 and 3 channels (Fig. 5a). On the other hand, when the flow rates of the buffer solution were increased to 1 $\mu\text{L}/\text{min}$ and 5 $\mu\text{L}/\text{min}$, the microbeads passed through the branch 1 and 2 channels and the branch 1 channel, respectively [Fig. 5(b) and (c)]. It was concluded that

the behavior of the microbeads after passing through the pinched channel was determined by competition between the inertia and the hydrodynamic force caused by the introduction of the buffer solution.

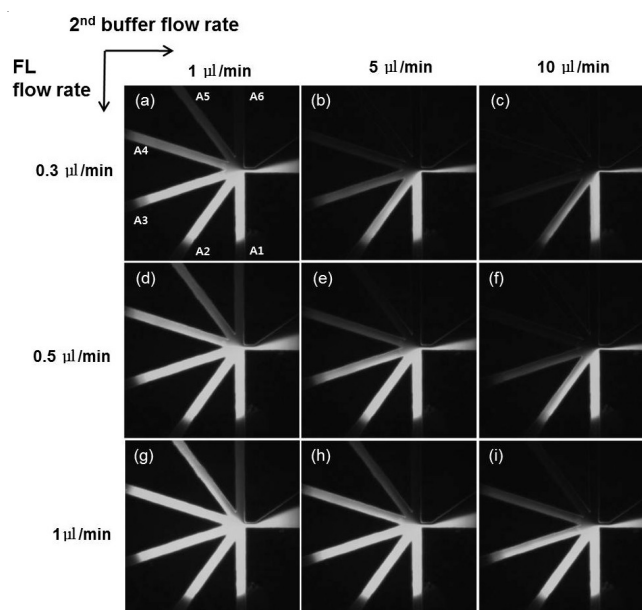


Fig. 4. Fluorescence image in the separation region with a change in flow rate of the main stream after mixing and the 2nd buffer solution

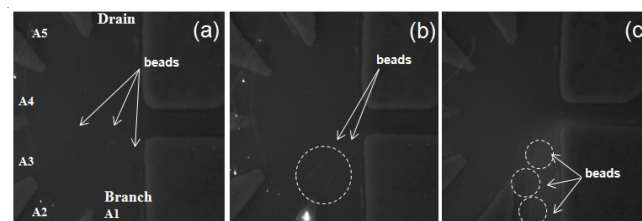


Fig. 5. The motions of microbeads after passing through the pinched channel under the different flow rates of buffer solution (a) 0.5 $\mu\text{L}/\text{min}$, (b) 1 $\mu\text{L}/\text{min}$ and (c) 5 $\mu\text{L}/\text{min}$

Conclusion

Low-temperature co-fired ceramic process combined with photolithography was proposed for use in the fabrication of a ceramic-based microfluidic device that included a passive mixer and separator. Two types of solutions in the mixing area were well mixed by diffusion at the interface of the laminar flow showing a maximum mixing efficiency of 97.3 %. The separation of microbeads in the ceramic-based device with a pinched channel could be easily controlled by changing the flow rate of the 2nd buffer solution. The findings confirm that the efficiency of mixing and separation of ceramic-based microfluidic devices was readily achieved using only passive operation. Considering the unique properties of the low-temperature co-fired ceramic material and its related process, it represents a potentially promising candidate for the integration of a microfluidic component in a 3-dimensional structure.

ACKNOWLEDGEMENTS

This work was supported from the R & D program by Korea Institute of Ceramic Engineering and Technology.

REFERENCES

1. M. Chudy, I. Grabowska, A.F.- Szymanska, D. Stadnik, I. Wyzkiewicz, P. Ciosek, E. Jedrych, M. Juchniewicz, M. Skolimowski, K. Ziolkowska and R. Kwapiszewski, *Anal. Bioanal. Chem.*, **395**, 647 (2009).
2. M. Yamada and M. Seki, *Anal. Chem.*, **76**, 895 (2004).
3. S. Badilescu and M. Packirisamy, *Polymers*, **4**, 1278 (2012).
4. J. Chen, J. Li and Y. Sun, *Lab. Chip*, **12**, 1753 (2012).
5. R. Guldiken, M. Chan Jo, N.D. Gallant, U. Demirci and J. Zhe, *Sensors*, **12**, 905 (2012).
6. W.L. Zhang and R.E. Eitel, *Int. J. Appl. Ceram. Technol.*, **9**, 60 (2012).
7. M.R. Gongora-Rubio, M.B.A. Fontes, Z.M. da Rocha, E.M. Richter and L. Angnes, *Sens. Actuators B*, **103**, 468 (2004).
8. P. Bemnowicz and L.J. Golonka, *J. Eur. Ceram. Soc.*, **30**, 743 (2010).
9. M. Wu and R.A. Yetter, *J. Micromech. Microeng.*, **18**, 125016 (2008).
10. M.A. Ansari, K. Kim, K. Anwar and S.M. Kim, *J. Micromech. Microeng.*, **20**, 055007 (2010).
11. O. Shardt, S.K. Mitra and J.J. Derksen, *Chem. Eng. Sci.*, **75**, 106 (2012).
12. J. Takagi, M. Yamada, M. Yasuda and M. Seki, *Lab Chip*, **5**, 778 (2005).
13. J. Choi, Y.J. Yoon, Y.-S. Choi, H.T. Kim, J. Kim, J.-H. Lee and J.-h. Kim, *J. Ceram. Proc. Res.*, **12**, 146 (2011).